Far-infrared spectroscopy on oriented films of dry and hydrated DNA

A. Wittlin,* L. Genzel, F. Kremer,† S. Häseler, and A. Poglitsch
Max-Planck-Institut für Festkörperforschung, Heisenbergstrasse 1, Postfach 80 06 65, D-7000 Stuttgart 80, Federal Republic of Germany

A. Rupprecht
Department of Physical Chemistry, University of Stockholm, Arrhenius Laboratory, S-106 91 Stockholm, Sweden
(Received 2 December 1985)

Far-infrared measurements, between 3 and 450 cm^{-1}, of absorption spectra of highly oriented films of Li-DNA and Na-DNA in the temperature range 5—300 K are reported. Five low-frequency infrared-active vibrational modes are observed. The lowest infrared-active mode at 45 cm^{-1} for Li-DNA and 41 cm^{-1} for Na-DNA, as observed for the first time, is found to soften upon sample hydration. Studies of the hydration-induced absorption at the low-frequency end of the spectrum also show a pronounced absorption band at about 10 cm^{-1} that is attributed to relaxation processes. Based on a simple lattice-dynamics model, the description of low-lying vibrational modes of DNA is presented. Eigenvectors of the lowest infrared-active and Raman-active modes are calculated. In addition, the model semiquantitatively describes the influence of hydration on mode frequencies.

INTRODUCTION

Studies of the molecular dynamics and structure of nucleic acids are of general importance for the understanding of their functions. As such they have been the subject of several theoretical and experimental investigations.[1–8] Among them are spectroscopic studies,[2,5–8] predominantly of DNA solutions in the microwave[8] and optical[5] frequency ranges. Studies in the infrared were limited to dry or slightly hydrated DNA fibers[2] or, more recently, to oriented films.[7] Most of these studies have been carried out by means of Raman spectroscopy and very few far-infrared spectroscopic results are available.[6] In the case of hydrated samples, far-infrared studies are particularly difficult due to the strong water absorption extending over most of the far-infrared range. Notwithstanding, far-infrared studies provide direct information about the dielectric properties of the investigated materials.

The main purpose of this study is to determine the frequencies of low-lying (3—450 cm^{-1}) infrared modes of highly oriented films[9] of Na-DNA and Li-DNA. In order to investigate the mechanisms of water binding to DNA, studies of the hydration dependence of the position of the low-lying modes are performed. The present study extends down to the microwave region, usually inaccessible by Raman studies.[7] A theoretical model of lattice dynamics is presented. The description of low-lying vibrational modes of DNA is presented and the assignment of the lowest-lying Raman-active modes as previously reported,[2] is discussed. Additionally, this model can, in a semiquantitative way, predict the influence of hydration on the far-infrared spectra.

EXPERIMENTAL

The oriented DNA samples are cut out from 40-mm-wide films of oriented calf-thymus DNA (Worthington Biochemical Co.) prepared with a wet spinning method.[9] A large spinneret with 1600 cylindrical channels (80 μm diameter) allows the use of a higher feed rate of the DNA solution (90 ml/h) in order to reduce the spinning time. X-ray diffraction patterns of the DNA films taken at 75% relative humidity (rh),[10] reveal a high degree of film orientation. While no direct measurements of the DNA-chain-lengths distribution were made, the gel electroforesis studies of very similar DNA (Ref. 11) reveal the typical chain length in the range between 15 000 and 30 000 base pairs.[12]

The present study covers the frequency range between 3 and 450 cm^{-1}. Four different spectroscopic techniques are used. At the low end of the wave-number range (3—5 cm^{-1}) the measurements of the temperature dependence of the absorption coefficient are performed with the oversized-cavity technique.[13] This technique allows us to measure only the extinction coefficient k. Therefore the index of refraction n is determined with a polarized-double-beam microwave interferometer.[14] Although not suitable at the moment for temperature-dependent measurements, the interferometer provides high-accuracy dielectric data in the range between 1 and 11 cm^{-1}. Backward-wave oscillators (Siemens A.G., model nos. RW0110 and RW0170) are used as radiation sources at wave numbers lower than 5 cm^{-1} and frequency multipliers above that range. A liquid-helium-cooled InSb bolometer (QMC) is used as a detector.

In the range between 5 and 450 cm^{-1} two Fourier-transform spectrometers (FTS) are used. A lamellar-grating instrument[15] measures the spectrum between 5 and 50 cm^{-1} and allows measurements of the samples at various humidities. A commercial FTS (Bruker IFS113) is used for the range between 20 and 450 cm^{-1} for measurements of vacuum-dried samples in the temperature range between 5 and 300 K.

A special sample cell has been constructed for the

FTS-ir study of the hydration-dependent absorption. A cylindrically shaped cell (Fig. 1) has two polyethylene-foil windows of 6 μm thickness. By design the windows are not parallel to each other and are separated by about 30 mm. No interferences between or within the cell windows are observed. The sample is mounted inside the cylinder on a metallic frame with an aperture of 15 mm. The whole cell is connected with polyethylene tubes to a closed circuit in which the relative humidity of the air can be continuously varied. A membrane pump forces the continuous flow of the predetermined humid air through the sample cell. To adjust the relative humidity a two-circuit system is used (Fig. 1). Circuit I contains the sample cell, humidity meter, membrane pump, and air-mixing glass cylinder [(2) in Fig. 1]. The second circuit includes another pump, humidity meter, and glass cylinder filled with an H_2O or D_2O salt solution [(3) in Fig. 1]. In order to change the relative humidity in the sample chamber the relative humidity in circuit II is adjusted under the control of the moisture meter. The valves control the flow through the sample cell. In order to dry the sample, the glass container with water is replaced by a container with a drying agent. The system allows the change of relative humidity in the sample cell continuously from less than 0.5% to 90% for both H_2O and D_2O. The equilibrium conditions within the sample cell are determined by monitoring the value of the humidity in the cell and monitoring the time dependence of the sample transmittance corresponding to the white-light position of the FTS.

Transmittance decreases upon sample hydration, and at constant humidity reaches some equilibrium value. The typical time constant at rh of $\leq 40\%$ is approximately 1 h. For the vacuum-dry sample case, in which one is free from errors in rh determination, white-light transmittance after several cycles of changes of sample humidity is reproducible to approximately 1%. The water uptake of the DNA films at different levels of hydration is measured by weighing. The hydration-induced variations in the thickness of the DNA films are determined microscopically. Due to the sample swelling upon hydration[16] and irreversible changes of its shape at humidities higher than 95%, the level of hydration in this study is limited to 90%.

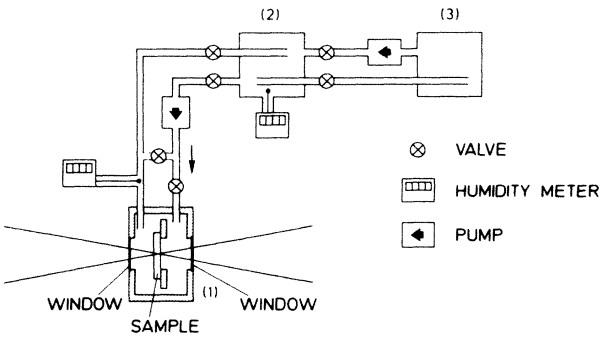

FIG. 1. Experimental design for a controlled-humidity far-infrared sample cell. (1) sample cell, (2) air mixing chamber, (3) constant humidity chamber.

TABLE I. Sample parameters of the oriented DNA films. Regarding the dry state see Ref. 19.

	Li-DNA	Na-DNA
Thickness	44 μm	48 μm
Salt content (g salt)/100 g dry weight	4.5 wt.% LiCl	1 wt.% NaCl
Conformation		
dry state	bases partly disordered	bases partly disordered
75% rh	*B* form	*A* form
90% rh	*B* form	*A*-*B* mixture

RESULTS

The sample parameters of Li-DNA and Na-DNA are presented in Table I. The samples are vacuum-dried, self-supporting films. The transmission spectra of Li-DNA and Na-DNA are shown in Fig. 2 and Fig. 3. The measurements are carried out at 5, 77, and 300 K. The transmission between 5 and 77 K is not significantly changed while at room temperature the transmission shows an overall decrease which may be attributed to multiphonon difference processes which freeze out upon cooling. Furthermore, the general shape of the spectrum is almost temperature independent. The transmission spectrum is measured for the electrical vector of the electromagnetic field both parallel and perpendicular to the DNA chain orientation. An anisotropy is observed only at higher frequencies and it is very weak. Therefore, only the spectra corresponding to the perpendicular orientation are shown.

In order to analyze the transmission results shown in Figs. 2 and 3 a multioscillator fit is performed.[17] The complex dielectric permittivity is expressed as

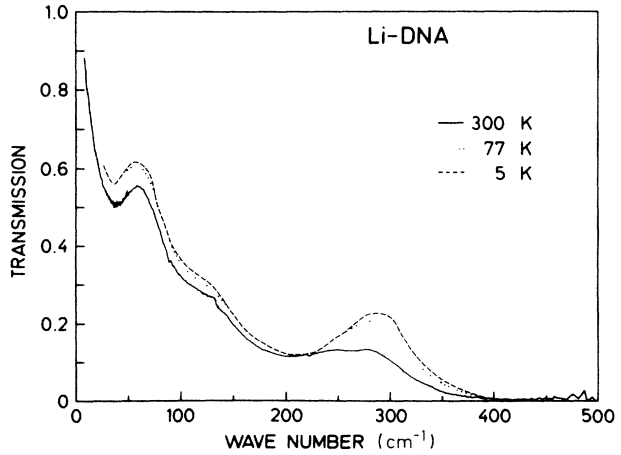

FIG. 2. Transmission spectrum of a vacuum-dried Li-DNA film of 44 μm thickness. The molecular axis is oriented perpendicular to the E vector of incident light. Results for parallel orientation do not differ within the experimental error.

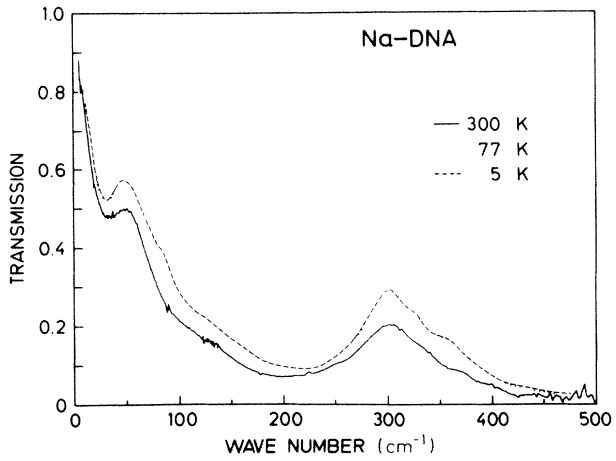

FIG. 3. Transmission spectrum of a vacuum-dried Na-DNA film of 48 μm thickness. Orientation as in Fig. 2.

$$\epsilon(\nu)=\epsilon_\infty+\sum_k \frac{S_k\nu_k^2}{\nu_k^2-\nu^2-i\nu\gamma_k}, \quad (1)$$

where ϵ_∞ is the high-frequency dielectric constant, S_k, ν_k, and γ_k are the oscillator strength, eigenfrequency, and the damping constant, respectively, of the kth oscillator mode. Five oscillators are used in Eq. (1) to fit the *transmission* data. The index of refraction n and extinction coefficient k are related to the real and imaginary part of the permittivity by the well-known equations

$$n=\left[\frac{|\epsilon|+\epsilon'}{2}\right]^{1/2}, \quad k=\left[\frac{|\epsilon|-\epsilon'}{2}\right]^{1/2}, \quad (2)$$

where $\epsilon=\epsilon'+i\epsilon''$. The calculated value of n and k for Li-DNA and Na-DNA are shown in Figs. 4 and 5, respectively. The value of the index of refraction $n=1.9\pm0.1$ for this calculation is taken from microwave measurements at 5.89 cm^{-1} at humidities less than 1% for both Li-DNA and Na-DNA. The values of the parameters S_k,ν_k,γ_k are shown in Table II.

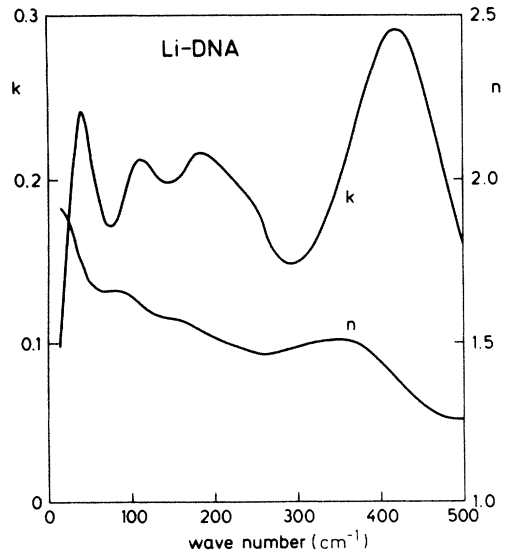

FIG. 4. Index of refraction and extinction coefficient for Li-DNA films, calculated from results presented in Fig. 2.

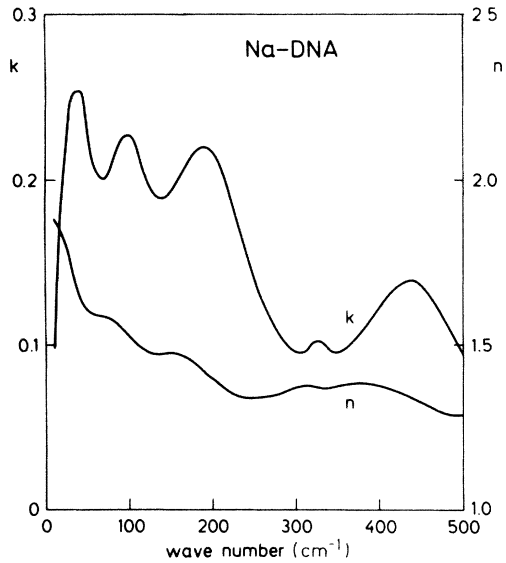

FIG. 5. Index of refraction and extinction coefficient for Na-DNA films, calculated for results presented in Fig. 3.

The influence of the sample hydration on the far-infrared spectra from 3 to 50 cm^{-1} is studied in the range of humidities 0–90 % at room temperature. The spectra of the extinction coefficient as a function of frequency for both types of DNA at different humidities are shown in Figs. 6 and 7. The values of the extinction coefficient are calculated from the exact formula for transmission through a plane-parallel slab.[18] Data for frequencies lower than 10 cm^{-1} are obtained from microwave measurements. Table III presents the water uptake at different hydration levels for Li-DNA and Na-DNA. Those results are slightly different from previously published data;[19] however, the difference may be attributed to the calibration errors of the humidity meters ($\pm2\%$). In addition, the influence of the hydration on the complex index

TABLE II. Parameters of the multioscillator fit for data shown in Figs. 2 and 3.

	ν_i (cm^{-1})	S_i	γ_I (cm^{-1})
Li-DNA	45	0.88	60
	111	0.22	70
	195	0.34	170
	245	0.25	60
	420	0.32	60
Na-DNA	41	0.98	60
	100	0.28	70
	200	0.37	140
	325	0.034	25
	444	0.13	175

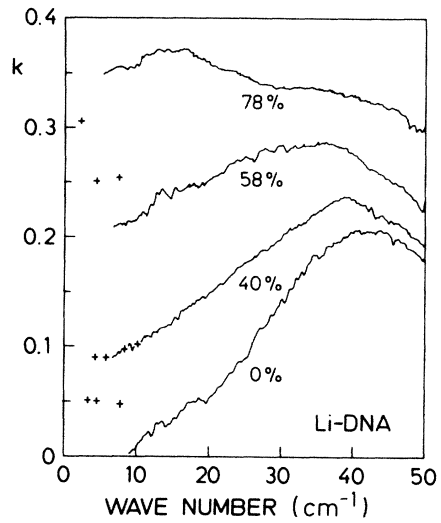

FIG. 6. Extinction coefficient as a function of frequency for Li-DNA films (not the same sample as in Fig. 2) at different humidities at 300 K. Microwave measurements are indicated by crosses (Table IV).

of refraction is studied at wave numbers below 6 cm^{-1}. A pronounced increase of the extinction coefficient k and of the index of refraction n with increased hydration is observed. Results are shown in Table IV. Furthermore, the microwave absorption of DNA films is also studied at low temperatures. The results for Na-DNA are shown in Fig. 8.

THEORY AND DISCUSSION

The lattice dynamics of DNA double helices has been calculated by Prohofsky and collaborators.[1,20] In these

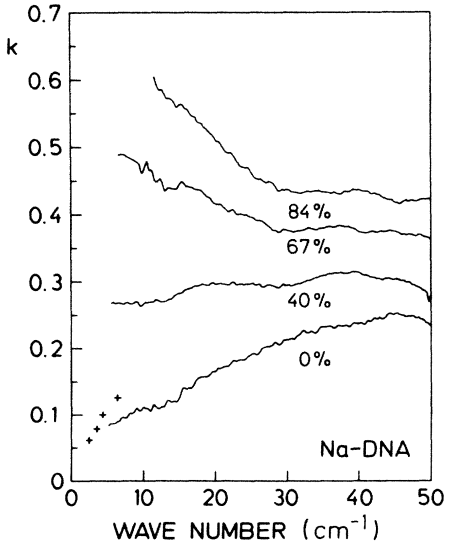

FIG. 7. Extinction coefficient as a function of frequency for (not the same sample as in Fig. 3) Na-DNA films at different humidities at 300 K. Microwave measurements are indicated by crosses.

TABLE III. Measured water uptake for Li-DNA and Na-DNA films.

rh (%)	Mass increase (%) Li-DNA	Na-DNA
42	19	19
90	97	108

calculations the full symmetry of DNA is exploited and all nonhydrogen atoms of the nucleotide pair are explicitly taken into account. Short-range force constants were refined to obtain agreement with low-frequency Raman data. Additionally, an effective long-range interaction was introduced to fit the observed compressional sound speed. This approach is very detailed and currently the most accurate model. However, due to the complexity of the calculations involved, the long-wavelength modes, such as translational vibrations of large molecular groups, are not easily visualized. Therefore in this paper a much simpler calculation is presented. It is based on lattice dynamics in the harmonic approximation and is restricted to the lowest infrared-active and Raman-active modes. Although several simplifications and approximations are made compared to the model presented in Refs. 1 and 20, the present model retains the substructure necessary to obtain the eigenvectors of the lowest modes. The unit cell of the linear-chain model consists of two identical nucleotides as shown in Fig. 9. In the rigid molecule approximation, molecular groups are represented by their centers of mass, coupled by central forces. Internal degrees of freedom, corresponding to high-frequency modes, are neglected. For each nucleotide the PO_4, counterion and 5'-CH_2 group are represented by m_1,[21] the sugar ring is represented by m_2, and the base by m_3, which represents the average mass of the four major bases existing in natural DNA. This model considers only displacements parallel to the helix axis and it is assumed that there is no coupling between motions in different directions. Such an approximation is really good only for the wave-vector $q=0$ modes. Furthermore, the effect of the chain helicity

TABLE IV. Microwave measurements of index of refraction and extinction coefficient of Li-DNA at three different humidities.

ν (cm^{-1})	rh %	n	k
4.00		1.91	0.052
5.04	8	1.93	0.047
5.89		1.90	0.034
4.00		2.0	0.076
5.04	36	2.1	0.070
5.89		1.99	0.084
4.00		2.22	0.314
5.04	78	2.12	0.252
5.89		2.13	0.257

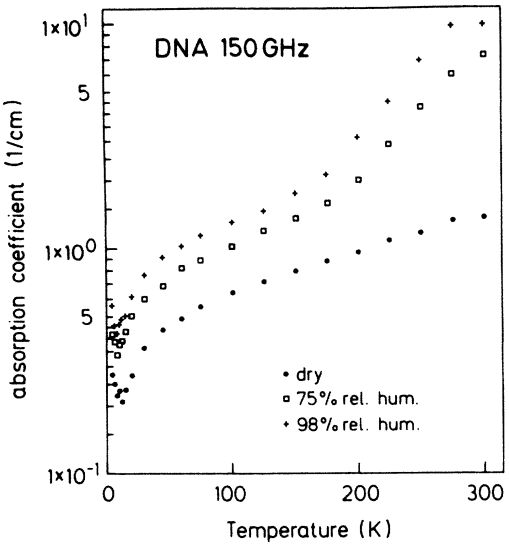

FIG. 8. Microwave-absorption coefficient of Li-DNA films at frequency 150 GHz as a function of temperature for three different sample humidities.

and the influence of the interhelical forces are neglected. For longitudinal vibrations in oriented and aligned DNA chains the interhelical forces correspond to the the bending of van der Waals forces and therefore are much weaker than intrahelical covalent bonds.

Since the masses of the model represent spatially extended molecular groups one has to expect that the displacements may be connected with torsional motions. Therefore the force constants used are "effective" force constants in the sense that they should be interpreted as a superposition of stretch, bend, and torsional type short-range forces,[1] including also some contribution from interhelical interactions. The displacement of the ith mass in the unit cell n from its equilibrium position is denoted as $x_{n,i}$ and $x'_{n,i}$, respectively, for the two strands (see Fig. 9). The equations of motion of the masses of the strand with unprimed x are[22]

$$m_1\ddot{x}_{n,1}=f_{12}(x_{n,2}-x_{n,1})-f_{12}(x_{n,1}-x_{n-1,2}), \tag{3}$$

$$m_2\ddot{x}_{n,2}=f_{12}(x_{n+1,1}-x_{n,2})-f_{12}(x_{n,2}-x_{n,1})+f_{23}(x_{n,3}-x_{n,2}), \tag{4}$$

$$m_3\ddot{x}_{n,3}=f_{33}(x_{n+1,3}-x_{n,3})-f_{33}(x_{n,3}-x_{n-1,3})-f_{23}(x_{n,3}-x_{n,2})+f_H(x'_{n,3}-x_{n,3}) . \tag{5}$$

The equations of motion of the strand with x' are completely analogous. The force constant f_H represents the bending force of the hydrogen bonds between adjacent bases. It couples the motions of the two strands of the helix. The chain is assumed to be finite with periodic boundary conditions. The solutions, therefore, can be considered as traveling waves with wave vector q. In the plane-waves ansatz the displacement $x_{n,i}$ can be written as[22]

$$x_{n,1}=A_1e^{-i(\omega t-2naq)}, \tag{6}$$

$$x_{n,2}=A_2e^{-i[\omega t-(2n+1)aq]}, \tag{7}$$

$$x_{n,3}=A_3e^{-i[\omega t-(2n+1)aq]} . \tag{8}$$

The expressions for $x'_{n,i}$ are completely analogous. Only real solutions are considered and the following abbreviations are used:

$$\Phi_1=2f_{12}-m_1\omega^2, \tag{9}$$

$$\Phi_2=2f_{12}+f_{23}-m_2\omega^2, \tag{10}$$

$$\Phi_3=2f_{33}+f_{23}-m_3\omega^2+f_H, \tag{11}$$

$$\Phi_{12}=2f_{12}\cos(aq), \tag{12}$$

$$\Phi_{33}=2f_{33}\cos(2aq) . \tag{13}$$

As a result the following amplitude ratios are obtained:

$$\frac{A_2}{A_1}=\frac{A'_2}{A'_1}=\frac{\phi_1}{\Phi_{12}},\quad \frac{A_3}{A_1}=\frac{A'_3}{A'_1}=\frac{\phi_1\phi_2-\phi_{12}^2}{f_{23}\Phi_{12}}, \tag{14}$$

$$\frac{A_3}{A_{1'}}=\frac{A'_3}{A_1}=\frac{(\phi_3-\phi_{33})(\phi_1\phi_2-\phi_{12}^2)-f_{23}^2\phi_1}{f_Hf_{23}\phi_{12}} . \tag{15}$$

The symmetry of these equations yields

$$A_i=\pm A'_i . \tag{16}$$

Equating the two independent solutions of Eqs. (14) and (15) yields the dispersion relation ω versus q in an implicit form:

$$(\phi_1\phi_2-\phi_{12}^2)(\phi_3-\phi_{33}\mp f_H)=f_{23}^2\phi_1, \tag{17}$$

where the upper sign in Eq. (17) corresponds to the upper sign in Eq. (16) and vice versa. Considering the expression for ϕ_3 in Eq. (11) one observes that f_H cancels for the upper $-$ sign in Eq. (17). This describes modes where both strands of the chain move in phase. These modes are labeled $+$.

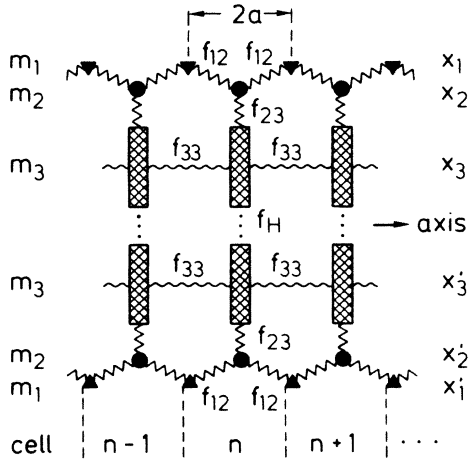

FIG. 9. Simplified lattice model of DNA. m_1 represents the PO_4 groups including 5'-CH_2, m_2 represents the sugar rings, and m_3 represents the bases.

Correspondingly, the − modes are those where the two strands of the chain move out of phase, as seen by the presence of the restoring force constant f_H. If the charge distribution on the two strands is identical, the − modes cannot yield a dipole moment at $q=0$ along the chain. Thus they are optically inactive but possibly Raman active. Equation (17) can be rewritten explicitly in powers of ω as

$$\omega^6+a_2^{\pm}\omega^4+a_1^{\pm}\omega^2+a_0^{\pm}=0\ . \tag{18}$$

The constants in Eq. (18) are

$$a_2^{\pm}=-[\omega_{12}^2+\omega_{23}^2+\omega_{33}^2\sin^2(aq)+\tfrac{1}{2}(\omega_H^2\mp\omega_H^2)]\ , \tag{19}$$

$$a_1^{\pm}=M_{23}\omega_{12}^2\omega_{23}^2[(m_2/m_3)^{1/2}+(m_3/m_1)^{1/2}M_{12}]+\tfrac{1}{2}(\omega_H^2\mp\omega_H^2)[\omega_{12}^2+(m_3/m_2)^{1/2}M_{23}\omega_{23}^2]$$
$$+\sin^2(aq)[\omega_{12}^2\omega_{33}^2+M_{12}^2\omega_{12}^4+(m_3/m_2)^{1/2}M_{23}\omega_{23}^2\omega_{33}^2]\ , \tag{20}$$

$$a_0^{\pm}=-M_{12}\omega_{12}^2\sin^2(aq)\{M_{23}\omega_{23}^2[(m_2/m_3)^{1/2}M_{12}\omega_{12}^2+(m_3/m_1)^{1/2}\omega_{33}^2]M_{12}\omega_{12}^2\omega_{33}^2\sin^2(aq)\}$$
$$-\tfrac{1}{2}(\omega_H^2\mp\omega_H^2)M_{12}\omega_{12}^2[(m_3/m_1)^{1/2}M_{23}\omega_{23}^2+M_{12}\omega_{12}^2\sin^2(aq)]\ , \tag{21}$$

where the following abbreviations have been used:

$$\omega_{12}^2=\frac{2f_{12}}{\mu_{12}},\quad \omega_{23}^2=\frac{f_{23}}{\mu_{23}},\quad \omega_{33}^2=\frac{2f_{33}}{\mu_{33}},\quad \omega_H^2=\frac{f_H}{\mu_{33}}\ ,$$
$$\mu_{ij}=m_im_j/(m_i+m_j),\quad M_{ij}^2=\mu_{ij}/(m_i+m_j)\ , \tag{22}$$
$$i,j=1,2,3\ .$$

Equation (17) yields now six lattice-dynamical branches: one acoustical branch and two optical branches for the + modes and three optical branches for the − modes. Considering the acoustic branch in the limit $q\to 0$ one finds the sound velocity:

$$v_s=2a\,[(f_{33}+\tfrac{1}{2}f_{12})/(m_1+m_2+m_3)]^{1/2}\ . \tag{23}$$

The sound velocity[23] v_s and the lattice constant[24] $2a$ are known from experiments. Equation (23) allows us then to eliminate one of the force constants f_{33} or f_{12}. In the present approach the long-range interactions between bases and dielectric screening as used by Prohofsky *et al.*[1] are not explicitly included. From Eq. (18) the lowest − mode at $q=0$ has in the limit of $\omega_H^2\ll\omega_{12}^2,\omega_{23}^2,\omega_{33}^2$ the frequency

$$\omega_{R0}^2\approx\frac{f_H}{\frac{1}{2}(m_1+m_2+m_3)}\ . \tag{24}$$

The denominator in Eq. (24) represents just the reduced mass of the DNA unit cell with respect to a vibration of the two strands of the double chain against each other along the axis. This eigenvector-eigenvalue assignment has been previously made by Prohofsky *et al.*[1] Notice that such a mode is infrared inactive in the dipole approximation within our model. From the symmetry of the model one can see that f_{23} does not enter the expression for v_s. Furthermore, due to the symmetry the value of f_{33} does not affect the $q=0$ optical modes. However, f_{33} is essential for the acoustic branch. The force constant f_{12} appears in Eq. (23) with coefficient $\frac{1}{2}$ because two such springs are in series along the DNA chain within the unit cell.

The values of the force constants f_{12} and f_{23} are obtained from the fit of the two lowest $q=0$ optical modes (in + branches) to our far-infrared spectroscopic measurements. It is assumed that there are no other optically active modes of still lower frequencies. In fact, measurements down to 1.6 cm^{-1} in the millimeter-wave region do not show further vibrational absorption. The value of the force constant f_H is obtained from the fit of the lowest − mode to the lowest Raman-active mode. Urabe *et al.*[2] and Lindsay *et al.*[7] have observed a hydration-sensitive, Raman-active mode in Na-DNA at about 25 cm^{-1}. Recently Lindsay *et al.*[7] have also reported an even lower mode at 15 cm^{-1} and observing the next one at 28 cm^{-1}. Within this model two values of f_H are considered corresponding to the two lowest, hydration-sensitive Raman-active modes. If we assume 15 cm^{-1} as correponding to the lowest − mode, f_H is found to be 0.025 mdyn/Å. Alternatively, the 28-cm^{-1} mode yields a value of f_H that is an order of magnitude higher. Since in this model f_H represents a bending force constant for hydrogen bonds, the assignment of the lowest mode at $\nu_R\approx 15$ cm^{-1} is reasonable. The mode observed in Raman scattering at 28 cm^{-1} is then not described by this model.

Within the framework of the model presented above, only six low-frequency modes, corresponding to the lowest longitudinal vibrations are described. Two of them correspond to the optical modes observed in far-infrared experiment. However,there may be additional degrees of freedom, e.g., torsional motions, which could possibly explain the low-frequency Raman mode at 28 cm^{-1}. Also this simple model predicts polarization dependences which are not observed in the experiment. This can be attributed to the chain helicity and partial disorder of DNA films.

It should be stressed that while the $q=0$ mode frequencies are fitted to the experimental ones, the mode symmetries and their eigenvectors result solely from the properties of the assumed lattice model. All parameters used for the calculations are shown in Table V and the dispersion curves obtained from Eq. (18) are shown in Fig. 10 (solid lines). Analysis of eigenvectors shows that the zone-boundary modes are vibrations of essentially only one of the masses, namely, m_1 for the lowest branch, m_2 for the next one, and m_3 for the highest. Masses in adjacent cells vibrate out of phase.

Upon hydration water molecules are bound to the molecular groups forming the DNA chains. The amount and the positions of the bound water molecules have been

TABLE V. Parameters of the model calculation. Masses in amu, v_s in 10^5 cm/s, a in Å, force constants in mdyne/Å, frequencies in cm^{-1}. For hydration, mass loading by water molecules is as follows: 7 H_2O on m_1, 5 H_2O on m_2, and 4 H_2O on m_3. The frequencies given were calculated from Eq. (22). They are not independent parameters.

	Dry Li-DNA	90% rh DNA
m_1	116	242
m_2	69	159
m_3	129	201
v_s	3.4	1.9
$2a$	2.92	3.36
f_{12}	0.125	0.125
f_{23}	0.121	0.121
f_{33}	0.629	0.257
f_H	0.025	0.025
ν_{12}	98.8	66.4
ν_{23}	67.5	48.0
ν_{33}	182	93.2
ν_H	25.6	20.5

studied theoretically by Corongiu and Clementi.[25] Two different types of reversible water-binding mechanisms have been found. For the initial hydration chemically bound water is found on the molecular groups, i.e., m_1, m_2, and m_3. With further hydration van der Waals bound water occurs. For the present study, limited to relative humidities less than 90%, only the former type of water is taken into account. Such an assumption is consistent with our measurements of water uptake by DNA upon hydration. The measured amount of water bound to

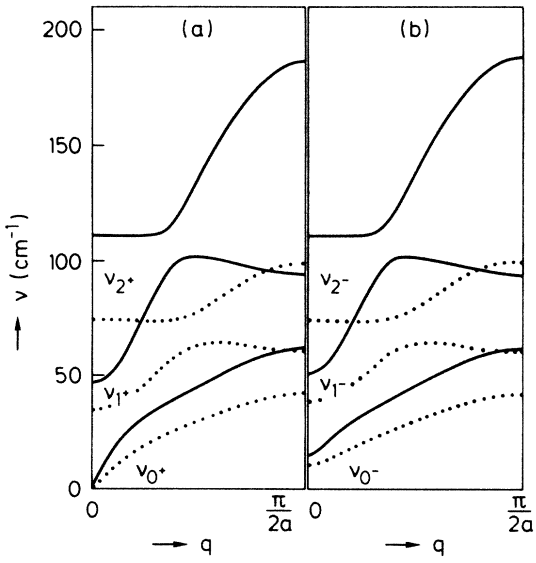

FIG. 10. Calculated dispersion curves for Li-DNA at two different [0% (solid lines) and ≃90% (dotted lines)] humidities; (a) + modes, (b) − modes. Parameters for calculations are given in Table V.

TABLE VI. Eigenfrequencies and eigenvectors of the $q=0$ modes for Li-DNA. The mode eigenfrequencies, given in wave numbers, are labeled ν_0, ν_1, and ν_2 according to increasing values. The displacement of mass m_1 is normalized to unity. The numbers of this table are based on the parameters given in Table V. Note that in the present model the displacements of the second helix are equal to those of the first helix for the + modes while they are opposite for the − modes.

	Dry DNA		90% rh DNA	
	+ modes	− modes	+ modes	− modes
ν_0	0	15.0	0	10.7
x_1	1	1	1	1
x_2	1	0.94	1	0.94
x_3	1	1.09	1	1.05
ν_1	46.5	50.7	35.1	38.9
x_1	1	1	1	1
x_2	0.41	0.29	0.30	0.13
x_3	−1.12	−0.47	−1.44	−0.27
ν_2	110	110	74.1	74.2
x_1	1	1	1	1
x_2	−2.34	−2.34	−2.14	−2.15
x_3	0.35	0.35	0.49	0.49

DNA agrees well with values obtained in Ref. 25 for chemically bound water in Na-DNA. There are no theoretical results available for the case of Li-DNA but we assume that the Na-DNA results could be applied here as well. It is recognized, however, that conformational *A-B* changes upon hydration and different salt amounts in the case of Na-DNA may lead to qualitatively different results at high hydration levels.[2,19,20] Furthermore, we assume that the principal effects of hydration on the lattice dynamics are an increase of m_1, m_2 and m_3 due to mass loading by water molecules and a change of the lattice-spacing constant.

Because of $m_i \gg m_{H_2O}, m_{D_2O}$, the increase of the masses is almost the same for deuterated samples and indeed spectra of H_2O and D_2O hydrated DNA do not differ. Within this model, if the value of sound velocity v_s at different hydrations is taken from the experiment and if f_{12}, f_{23}, and f_H are assumed unchanged upon hydration, f_{33} is found to increase weakly. However, the increased lattice constant $2a$ associated with the *A*-to-*B* transition[24] results in a decrease in f_{33} as shown in Table V. Results of the calculation for a relative humidity of about 90% (dashed lines) are shown in Fig. 10 and in Table VI. The shifts to lower frequencies of the 47-cm^{-1} infrared and the 15-cm^{-1} Raman[7] modes upon hydration are in favorable agreement with calculations (Fig. 10). This effect is more pronounced for the Li-DNA data. For both Li-DNA and NA-DNA the absorption increases dramatically upon hydration at less than about 20 cm^{-1}. For higher hydrations the mode softening is effectively masked. Microwave studies of DNA films (Fig. 8) sug-

gest that this absorption results from relaxation-type processes. Such processes exist intrinsically in dry DNA and further relaxational processes due to water appear at higher hydration levels. In two earlier investigations on hydrated lysozyme[26] and polyamid[27] we have studied this effect in detail.

It is noteworthy that there are two effects occurring in the low-frequency ir spectroscopy of natural DNA which contains a statistical distribution of the possible base pairs. Firstly, all the observed absorption bands will be inhomogeneously broadened. Secondly, there is in fact no perfect structural periodicity along the helix axis. This kind of disorder causes a broad, polarization-independent disorder-induced one-phonon absorption which is temperature independent.[28]

CONCLUSIONS

The far-infrared and millimeter-wave absorption of oriented films of Li-DNA and Na-DNA are measured for the first time. Included in this investigation is the dependence of the spectra upon hydration. Of special interest is a low-frequency band around 47 cm^{-1} which shifts to lower frequencies with increasing hydration, an effect which has been found earlier in several studies of low-frequency Raman modes in DNA. A simple lattice-dynamical calculation demonstrates that this infrared band and the lowest-lying Raman band have distinctly different eigenvectors. The previous assignment of the lowest-lying Raman-active mode to 15 cm^{-1} is consistent with the model calculation. Moreover, model calculation shows that the mass loading of the molecular subunits of DNA by bound water molecules and the change in lattice constant associated with the conformational transition seem to be the main causes of the softening of the modes upon hydration.

ACKNOWLEDGMENTS

One of us (A.W.) would like to express his thanks to the Max-Planck-Gesellschaft for financial assistance. We thank Professor H. Bilz, Professor W. Peticolas, Professor E. Prohofsky, Dr. G. Edwards, and Dr. J. Powell for many helpful discussions. Assistance of Dr. G. Bechtold with computer programming and the assistance of Mr. W. König with the measurements is gratefully acknowledged.

---

*On leave of absence from Institute of Physics, Polish Academy of Sciences, Aleja Lotnikow 32, PL-02-668 Warszawa, Poland.

†Present address: Max-Planck-Institut für Polymerforschung, D-6500 Mainz, Federal Republic of Germany.

[1]K. V. Devi-Prasad and E. W. Prohofsky, Biopolymers **23**, 1795 (1984); see also E. W. Prohofsky, Phys. Rev. Lett. **54**, 607 (1985); S. M. Lindsay, J. W. Powell, E. W. Prohofsky, and K. V. Devi-Prasad, in *Structure and Dynamics of Nucleic Acids, Proteins and Membranes,* edited by F. Clementi and R. M. Sarma (Adenine, New York, 1985); Y. Gao, K. V. Devi-Prasad, and E. W. Prohofsky, J. Chem. Phys. **80**, 6291 (1984); Y. Kim, K. V. Devi-Prasad, and E. W. Prohofsky, Phys. Rev. B **32**, 5185 (1985).

[2]M. Urabe, H. Hayashi, Y. Tominaga, Y. Nishimura, K. Kubota, and M. Tsuboi, J. Chem. Phys. **82**, 531 (1985).

[3]H. Frauenfelder, Helv. Phys. Acta **57**, 165 (1984).

[4]A. J. Martin, Biopolymers **23**, 471 (1984).

[5]C. P. Beetz and G. Ascarelli, Biopolymers **21**, 1569 (1982).

[6]R. Giordano, F. Mallamace, N. Micali, F. Wanderlingh, G. Baldini, and S. Doglia, Phys. Rev. A **28**, 3581 (1983).

[7]S. M. Lindsay, J. W. Powell, and A. Rupprecht, Phys. Rev. Lett. **53**, 1853 (1984).

[8]G. S. Edwards, C. C. Davis, J. D. Saffer, and M. L. Swicord, Phys. Rev. Lett. **53**, 1284 (1984).

[9]A. Rupprecht, Acta Chem. Scand. **20**, 495 (1966); Biotechnol. Bioeng. **12**, 93 (1970).

[10]A. Rupprecht and B. Forslind, Biochim. Biophys. Acta **204**, 304 (1970).

[11]J. Powell (private communication).

[12]S. M. Lindsay and J. Powell, Biopolymers **22**, 2045 (1983).

[13]F. Kremer, A. Poglitsch, D. Böhme, and L. Genzel, in *Infrared and Millimeter Waves,* edited by K. Button (Academic, Orlando, Florida, 1984), Vol. 11.

[14]L. Genzel, A Poglitsch, and S. Häseler, Int. J. Infrared and Millimeter Waves **6**, 741 (1985).

[15]G. Bechtold, thesis, University of Karlsruhe, 1985.

[16]G. S. Edwards, L. Genzel, W. L. Peticolas, and A. Rupprecht, Biopolymers **25**, 223 (1986).

[17]S. Shen, L. Santo, and L. Genzel, Can. J. Spectrosc. **26**, 126 (1981).

[18]E. D. Palik and J. K. Furdyna, Rep. Prog. Phys. **33**, 1193 (1970).

[19]M. Falk, K. A. Hartman, and R. C. Lord, J. Am. Chem. Soc. **84**, 3843 (1962); **85**, 391 (1963).

[20]W. N. Mei, M. Kohli, E. W. Prohofsky, and L. L. Van Zandt, Biopolymers **20**, 833 (1981).

[21]According to Falk *et al.* (Ref. 19) the counterions are likely to be rather strongly associated with the phosphate groups.

[22]P. C. Painter, M. M. Coleman, and J. L. Koenig, *The Theory of Vibrational Spectroscopy and Its Application to Polymeric Materials* (Wiley, New York, 1982).

[23]G. Maret, R. Oldenbourg, G. Winterling, K. Dransfeld, and A. Rupprecht, Colloid Polymer Sci. **57**, 1017 (1979); see also M. B. Hakim, J. W. Powell, and S. M. Lindsay, Biopolymers **23**, 1185 (1984).

[24]R. E. Dickerson, Sci. Am. **249**, 87 (1983); see also J. Mol. Biol. **166**, 419 (1983).

[25]G. Corongiu and E. Clementi, Biopolymers **20**, 551 (1981); **20**, 2427 (1981); **21**, 763 (1982).

[26]A. Poglitsch, F. Kremer, and L. Genzel, J. Mol. Biol. **173**, 137 (1984).

[27]C. S. Nie, F. Kremer, A. Poglitsch, G. Bechtold, and L. Genzel, J. Polymer Sci. Polymer Phys. Ed. **23**, 1247 (1985).

[28]A. S. Barker and A. J. Sievers, Rev. Mod. Phys. **47**, Suppl. No. 2 (1975).